J Therm Anal Calorim (2017) 128:1093–1106
DOI 10.1007/s10973-016-5992-7

Crystallization and melting characteristics of iPP nucleated by a sustainable eggshell powder-supported β-nucleating agent

Yi Li[1] · Junjun Kong[2] · Shuangyang Xin[2] · Changyu Han[2] · Liguang Xiao[1]

Received: 20 May 2016 / Accepted: 19 November 2016 / Published online: 29 November 2016

Abstract The β-form crystals in isotactic polypropylene (iPP) are proved to be favorable and effective for developing general iPP plastics with high performance. Herein, sustainable eggshell power decorated with calcium pimelate (DES), an effective β-form nucleating agent for iPP, was fabricated via the interaction between pimelic acid and Ca^{2+} on the surface of eggshell powder at elevated temperature. DSC and FTIR analysis identified the reaction occurred and formation of calcium pimelate on surface of the eggshell powder. Then, the effects of the functionalized eggshell powder on the nonisothermal and isothermal crystallization behavior, melting characteristics and polymorph structures were investigated. From the nonisothermal crystallization experiments, the incorporation of supported β-form nucleator greatly enhanced the crystallization temperature of iPP. The content of β-form crystals (K_β) could reach a value as high as 87% at 5 mass% DES load. Moreover, the crystallization and melting characteristics of iPP nucleated by DES were not changed under multiple scan conditions with melt temperature range from 190 to 250 °C. Interestingly, from the investigation of isothermal crystallization and subsequent melting behavior, it was found that DES is a temperature-dependent selective nucleator for inducing iPP crystallization. Main α-form crystals or β-form crystals could form when using high or low crystallization temperatures, respectively. Particularly, these results demonstrated a possibility to tailor the ratio of α-form crystals to β-form crystals by simply choosing isothermal crystallization conditions. Then the crystallization mechanism based on thermodynamics and kinetics factors was further discussed.

Keywords Polypropylene · β-form crystals · Eggshell power

Introduction

Eggshell, consisting of approximately 94 mass% $CaCO_3$, 1 mass% $MgCO_3$, 1 mass% $Ca_3(PO_4)_2$ and 4 mass% organic component, supplies us with abundance $CaCO_3$ from sustainable bioresources [1, 2]. Eggshell, about 11 mass% in the overall weight of an egg, was directly disposed of as garbage in many industry usages such as food manufacturing every year. Therefore, the eggshells with characteristic of renewability, biodegradability, biocompatibility, unique physical properties have been paid great attention both from academy and from industry in recent years. The application of eggshell in many fields such as absorbing agents for dyes or heavy metals ions, nutrition for human has been extensively studied [3–6].

Another important application of eggshell is in polymer composites industry to serve as hard fillers. For example, bionanocomposites based on biopolymer and eggshell nanoparticles have been fabricated and physical properties such as thermal stability, tensile modulus and strength of the prepared nanocomposites had been pronouncedly enhanced compared with the neat biopolymer [7]. Rahman et al. [8] prepared a novel composite using soy protein as matrix and eggshell nanopowder as fillers. Due to well-dispersed eggshell nanoparticles in protein matrix,

✉ Changyu Han
cyhan@ciac.ac.cn

[1] College of Material Science and Engineering, Jilin Jianzhu University, Changchun 130118, China

[2] Key Laboratory of Polymer Ecomaterials, Changchun Institute of Applied Chemistry, Chinese Academy of Sciences, Changchun 130022, China

the composites exhibited important enhancement in mechanical and thermal properties. Thermoplastic native starch/eggshell particles and traditional $CaCO_3$ composites were also prepared. The composites incorporated with eggshell particles had higher biodegradation rates compared with those incorporated with traditional $CaCO_3$ [9]. In comparison with other polypropylene (PP) composites, the eggshell powder-filled isotactic polypropylene (iPP) composites have been one of the important research fields in recent years. Different proportions of chicken eggshell as biofiller for polypropylene (PP) composite were reported and compared with different particle sizes and proportions of commercial talc and $CaCO_3$ fillers by tensile test. The Young's modulus was improved with the increment of eggshell content, and this biofiller was better than all types of carbonate fillers with different particle sizes used.

Isotactic polypropylene (iPP) is a widely used general polymer with low manufacturing cost and excellent physical properties. It can form polymorphic structure with at least four basic crystalline forms, namely the monoclinic α-form, trigonal β-form, orthorhombic γ-form and a new ε-form crystal [10, 11]. In the past decades, iPP with β-form crystal structure (β-iPP) has been paid great attention owing to its excellent mechanical properties. Many β-form nucleating agents have been developed to increase the β-iPP content of β-nucleated iPP and further tailor the mechanical properties of iPP. For example, a β-nucleating agent based on a trisamide of trimesic acid was developed by Varga et al. [12]. Yang et al. [13] synthesized *N*,*N*′-dicyclohexyl-1,5-diamino-2,6-naphthalenedicarboxamide, a new β-form nucleating agent for iPP. This nucleating agent showed high β-iPP content. Subsequently, the same group supported this kind of β-form nucleating agent onto the surface of graphene oxide [14]. The β-iPP content of 73.6% could be obtained in the iPP nanocomposites, and simultaneous enhancement in the tensile strength and impact strength could be realized. Eggshell/β-PP biocomposite was prepared and evaluated. The results showed that the maximum β-iPP content of 0.99 in PP composites could be obtained. The impact strength of PP increased by 228% compared with pure PP [15]. Menyhárd et al. [16] compared different β-nucleators for isotactic polypropylene using DSC and temperature-modulated DSC (TMDSC) measurements. Yang et al. [17] compared the β-nucleation ability of two different β-form nucleating agents (one based on a rare earth complex and another based on a metal salts compound) for iPP and observed that the metal salts compound showed higher β-iPP content. Aryl amide derivative, an effective β-form nucleating agent for iPP, showed temperature-dependent selective crystallization behaviors as evidenced by X-ray determination and polarized optical microscopy observation [18]. Cadmium bicyclo[2.2.1]hept-5-ene-2,3-dicarboxylate was also found to be a highly active β-form nucleating agent for iPP, and β-iPP content could reach 87% with only 0.1% addition of such nucleating agent [19]. Mani et al. [20] regulated the crystallization and morphology of the β-polymorph of isotactic polypropylene based on carboxylate–alumoxane nucleating agents. Fu et al. [21] studied the combined effects of the matrix crystalline structure and amorphous chain mobility on the low-temperature toughness of iPP/ethylene–octene copolymer (POE) blends by β-modification and annealing. The results show that β-modification and annealing have synergistic effect on toughening the blend and reducing the POE content for effectively increasing the toughness in the temperature range used, as a result of the synergetic improvement in the matrix cavitation ability. Moreover, the dynamic and isothermal crystallization and subsequent melting characteristics of iPP-tungsten disulfide (iPP/IF-WS_2) nanocomposites incorporating a β-nucleating agent were investigated. The results show that when the dual additive system is employed, the nucleation ability on isotactic polypropylene depends not only on the nucleation efficiency and relative content of the individual α- and β-form nucleating agents, but also on the cooling rates and isothermal crystallization temperature employed [22, 23]. More recently, the impacts of both shear temperature and shear rate on both the self-assembled β-nucleating agent in the hosting iPP matrix and the subsequent crystallization of the hosting iPP matrix were studied. It was found that under static condition, β-NA could self-assemble into snowflake-like aggregate. Once shear was applied, three kinds of self-assembled aggregates could be developed prior to the crystallization of matrix depending on the applied shear temperatures [24].

In current work, via reaction of pimelic acid with Ca^{2+} on the surface of eggshell powder at elevated temperature, we prepared a sustainable eggshell powder decorated with a β-form nucleating surface (DES). Then the DES was incorporated into iPP matrix by melt processing. The thermal history, the content of the DES on the nonisothermal and isothermal crystallization and melting characteristics as well as the β-iPP content in iPP were investigated in detail. Moreover, nonisothermal and isothermal crystallization behavior, and melting characteristics of neat iPP and iPP incorporated with eggshell powder were also compared.

Experimental

Materials and samples preparation

Isotactic polypropylene (iPP) T30S, with the melt flow index (MFI) of 2.1 g 10 min^{-1} (200 °C, 2.16 kg) and density of 0.91 g cm^{-3}, was purchased from Dushanzi Co. Ltd., China. Pimelic acid (PA) was purchased from Aldrich, which was used as received. The chicken eggshell used was supplied by a small restaurant in Changchun city.

The eggshells were ground via a ball-milling machine. Before grinding, the eggshells were cleaned by deionized water to eliminate impurities and dried to constant weight. The obtained eggshell power (ES) had average particle size of around 2 um as observed by SEM shown in Fig. 1.

ES and PA were first homogenized by a homo-mixer at room temperature. The mixture was then laid aside at 120 °C to react for 30 min. The ES/PA mass ratio was fixed at 5/1.

Various iPP/DES composites were prepared via a melt mixing in an internal mixer (Haake Rheomix 600). The mixing temperature and speed were 180 °C and 60 rpm. Neat iPP and iPP/ES were mixed using the same conditions for comparison. Then various samples were compression-molded at 180 °C with around 0.1 mm thickness for characterization. The samples with various contents of DES or ES were denoted as iPP/DESX or iPP/ESX, where X is the DES or ES content in samples.

Characterizations

The particle size of the ES was estimated by a SEM (FEI Co., Eindhoven, Netherlands). Before SEM characterization, the ES was gold-sputtered.

FTIR spectra were determined by a spectrometer (BIO-Rad Win-IR). A resolution of 4 cm^{-1} with a range of 4000–500 cm^{-1} was used.

A Q20 differential scanning calorimeter (DSC) (TA Instruments, USA) was used to investigate the non-isothermal and isothermal crystallization behavior and melting characteristics of the samples. Temperature and enthalpy calibration was performed using an indium standard. A sample size of 5–8 mg was used for each DSC run, and the measurements were taken in a dry nitrogen atmosphere. The sample was first heated and equilibrated at 190 °C for 5 min to remove any thermal history. For nonisothermal measurements, the sample was cooled to 50 °C at different cooling rates and then reheated up to 190 °C at different heating rates to study the melting behavior and polymorphism. It is worth noting that all recorded crystallization and melt enthalpies were normalized according to the amount of iPP within the blends.

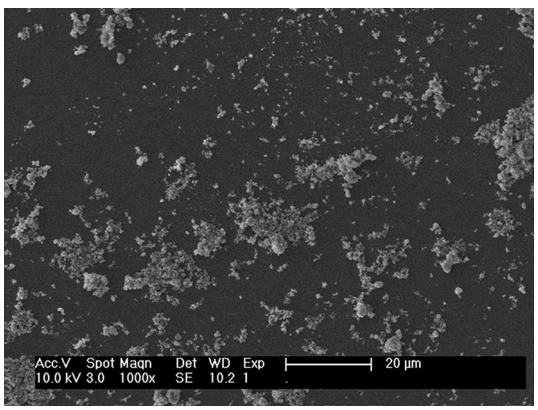

Fig. 1 SEM image of ES

For isothermal measurements, the sample was cooled from 190 °C to required crystallization temperatures and held isothermally until crystallization was complete as determined by a zero differential heat flux, and then reheated up to 190 °C at a heating rate of 10 °C min^{-1} to investigate the subsequent melting behavior and polymorphism.

Wide X-ray diffraction (WAXD) diagrams were determined by an X-ray diffractometer (Rigaku model Dmax 2500) with a Cu K_α radiation source (with parameters of $\lambda = 0.154$ nm, 200 mA, 40 kV). The scanning angle range and speed were 10–30° and 3° min^{-1}, respectively. To have the same thermal history as the DSC testing, the samples for WAXD testing were treated in the DSC cell by the same procedures as used for DSC testing. The relative content of the β-form crystals (K_β) was estimated according to the procedure developed by Turner-Jones et al., using the following equation: [14]

$$K_\beta = H_\beta/(H_{\alpha1} + H_{\alpha2} + H_{\alpha3} + H_\beta) \quad (1)$$

where H_{a1}, H_{a2} and H_{a3} are the intensities of (110), (040) and (130) diffraction peaks of the α-form crystals, which are correspond to $2\theta = 14.0°$, 17.1° and 18.7°, respectively. H_β is the intensity of (300) diffraction peak of the β-form crystals at $2\theta = 16.0°$

Results and discussion

Surface functionalization of ES

Since the main component of ES is $CaCO_3$, the Ca^{2+} on the surface of ES can react with PA when the reacting temperature is higher than the melting point of PA. Figure 2a shows the DSC curves of neat ES, PA and DES. It can be clearly seen from Fig. 2a that neat PA has a melting point located at 112 °C with an enthalpy of 222.7 J g^{-1}. However, the melting peak at 112 °C could not be found for DES sample, suggesting that PA reacted with the Ca^{2+} on the surface of ES to form calcium pimelate layer on the surface of ES. Moreover, FTIR spectroscopy was also applied to further identify the reaction between PA and the Ca^{2+} on the surface of ES. Before FTIR testing, the unreacted PA was eliminated by washing in acetone. As shown in Fig. 2b, the typical absorption peaks at 2900 cm^{-1} wavenumber for the PA could be clearly seen for the DES sample, indicating that the reaction occurred to form calcium pimelate, an effective β-form nucleating agent for iPP.

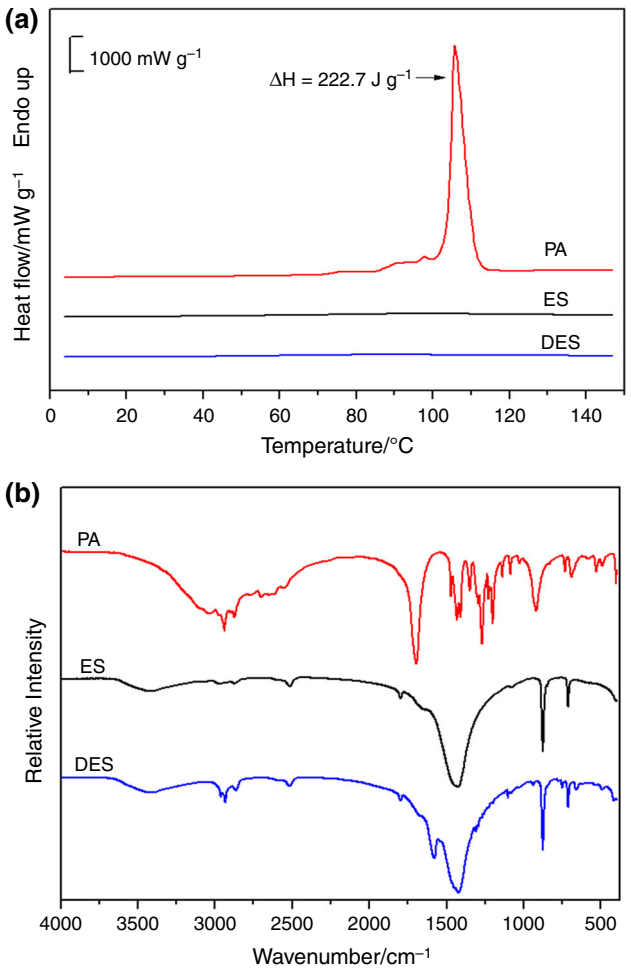

Fig. 2 DSC curves (heating rate of 10 °C min^{-1}) (**a**) and FTIR spectrum (**b**) of PA, ES and DES

Effect of ES and DES on nonisothermal crystallization and melting behaviors of iPP

The β-form nucleating agent containing ES and calcium pimelate, an active β-form nucleation component for iPP, was fabricated via supporting calcium pimelate onto the surface of ES. In the supporting process, PA and ES could react at temperature up to the melting point of PA to form the calcium pimelate, the β-form nucleating agent on ES surface. So the nonisothermal crystallization and melting behavior of iPP incorporated with ES and DES were investigated firstly. Figure 3 exhibits the nonisothermal crystallization and melting curves of iPP nucleated by DES and incorporated by ES at a cooling rate of 10 °C min^{-1}, and the corresponding data are summarized and presented in Table 1. As shown in Fig. 3a, incorporation of DES into iPP enhanced the crystallization temperature (T_c) of iPP greatly. However, ES had little effect on the T_c of iPP. Moreover, the melting behaviors of neat iPP and iPP nucleated by DES and iPP incorporated with ES exhibited much more different characteristics. As shown in Fig. 3b, for neat iPP and iPP incorporated with various contents of ES, one main melting peak was observed at around 161–166 °C corresponding to the melting of the α-phase [13], which indicated that main α-form crystals formed during the nonisothermal crystallization process. Moreover, a small peak at 140–145 °C corresponding to the melting of the β-phase could be also observed, indicating a small content of β-form crystals formed. This is in agreement with the XRD results below. However, for DES nucleated iPP, the main melting peak was shifted to approximately 150–153 °C, indicating main β-form crystals formed during the nonisothermal crystallization process [13]. Therefore, the DES can serve as a high effective and selective β-form nucleating agent for iPP under nonisothermal crystallization conditions.

To further understand the development of crystallization during the nonisothermal crystallization process, the Avrami model was applied to analyze the nonisothermal crystallization kinetics of neat iPP and iPP incorporated with 1 mass% ES and 1 mass% DES. The Avrami equation can be expressed as follows [25]:

$$\ln[-\ln(1 - X_t)] = \ln Z_t + n \ln t \quad (2)$$

where n is the Avrami exponent, Z_t is the crystallization rate constant involving nucleation and growth parameters, and X_t is the relative degree of crystallinity at crystallization time t. Avrami plots according to Eq. (2), $\ln[-\ln(1 - X_t)]$ versus $\ln t$, are shown in Fig. 4. It was obvious that the initial stage of crystallization of all samples followed the Avrami equation and held in the region from the beginning of crystallization to the roll-off to a secondary process. The deviation of the Avrami plots may have been due to spherulite impingement, which indicated that there was a slow secondary crystallization that continued long after its boundary was formed. The values of n determined from the slope of the selected plots are shown in Fig. 4. The n values were in the range of 2.8–3.6 for neat iPP and iPP incorporated with 1 mass% ES and DES. The slight difference of n values among these samples indicates that the incorporation of ES and DES into iPP matrix did not clearly change the crystallization mechanism during nonisothermal crystallization processes.

X-ray diffraction profiles of neat iPP, iPP nucleated by DES and filled by ES are shown in Fig. 5. The K_β values of various samples obtained from Eq. (1) are listed in Table 1. The K_β value of neat iPP was near to zero. The incorporation of ES and increase in the ES level slightly increased the K_β values of iPP. It should be noted that a K_β value of above 0.79 could be achieved for iPP nucleated by DES. These results further indicate that the DES that acted as an effective β-form nucleating agent has high β-form nucleation capability.

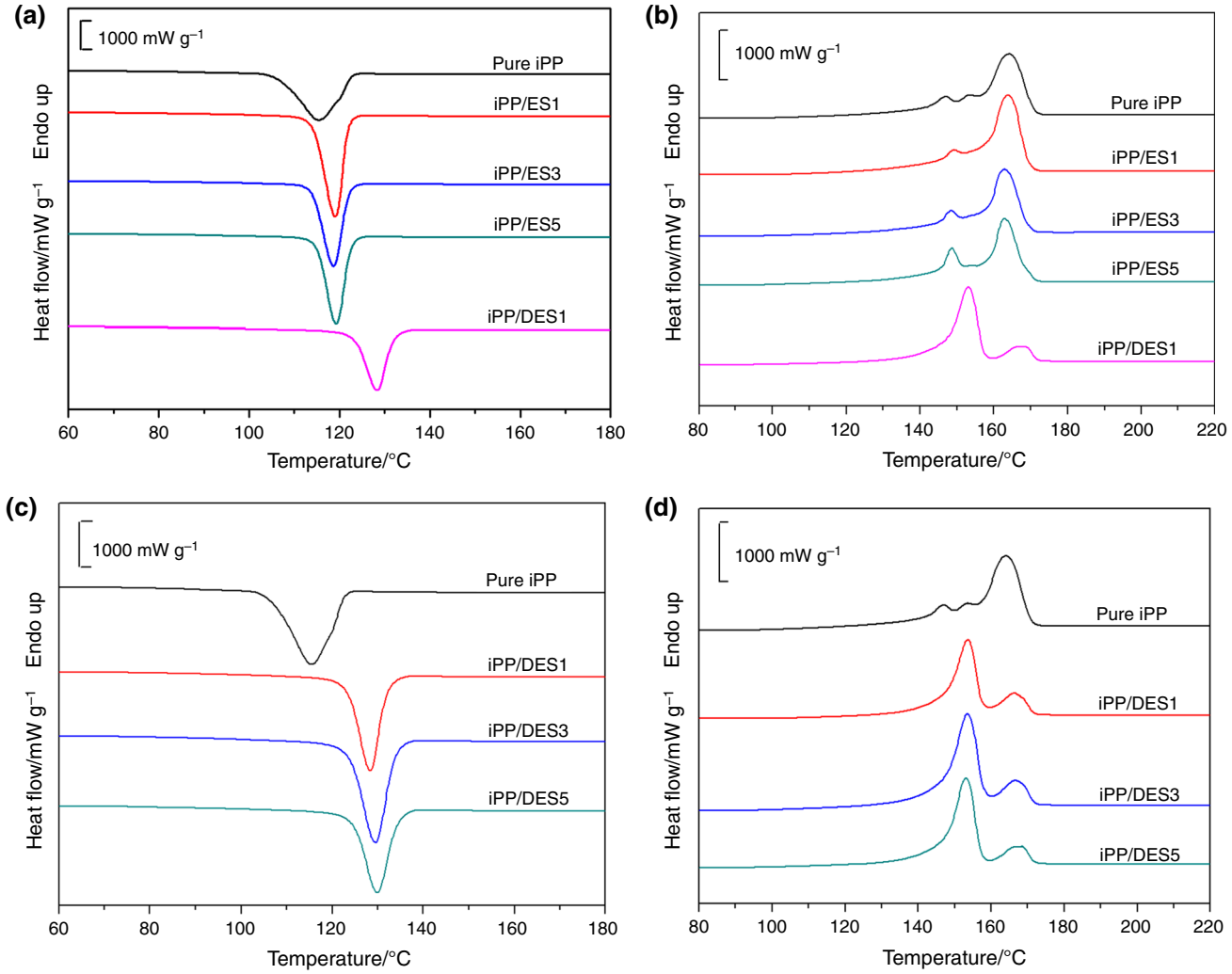

Fig. 3 Crystallization (**a**, **c**) and melting (**b**, **d**) plots for various samples with heating and cooling rate of 10 °C min^{-1}

Table 1 DSC crystallization and melt parameters for various samples

Sample	T_c/°C	ΔH_c/J g^{-1}	T_β/°C	ΔH_β/J g^{-1}	T_α/°C	ΔH_α/J g^{-1}	K_β
Pure iPP	115.5	106.8	146.7	3.5	164.5	48.4	0.05
iPP/ES1	119.1	104.0	149.0	2.4	164.0	50.0	0.13
iPP/ES3	118.7	98.7	148.3	3.9	163.1	48.3	0.20
iPP/ES5	119.3	99.9	148.6	8.2	163.1	44.2	0.36
iPP/DES1	128.4	105.4	153.6	52.8	166.6	12.4	0.79
iPP/DES3	129.5	102.6	153.5	69.1	167.0	11.9	0.81
iPP/DES5	129.9	105.0	153.1	70.1	168.6	11.5	0.87

Effect of DES contents on crystallization and melting behaviors of iPP

The crystallization and melting plots of iPP nucleated by different levels of DES are given in Fig. 3c, d, and the corresponding data are summarized and listed in Table 1. Apparently, the incorporation of DES pronouncedly enhanced the T_c of iPP. The T_c increased from 115.5 °C of neat iPP to 128.4 °C after incorporation of 1 mass% DES into iPP matrix, and the T_c of iPP further increased with an increase in the level of DES. Different from neat iPP, two melting peaks with one main melting peak at approximately 150–153 °C could be observed in the melting curves, again indicating that main β-form crystals form during the nonisothermal crystallization process. X-ray diffraction profiles of iPP nucleated by DES are shown in

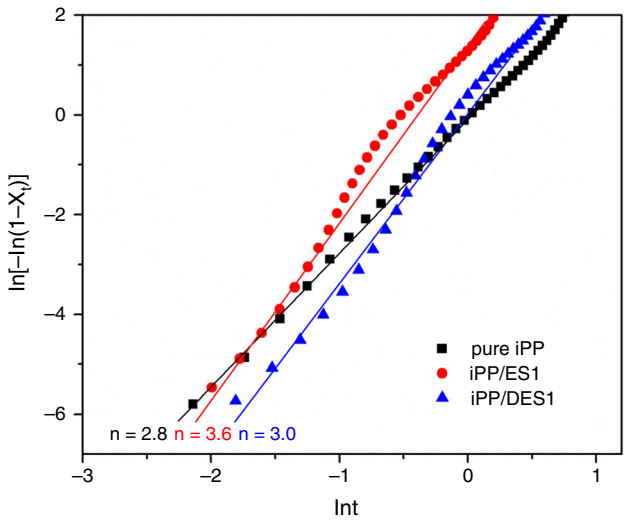

Fig. 4 Avrami plots of $\ln[-\ln(1 - X_t)]$ against $\ln t$ for the crystallization of (**a**) iPP, iPP/ES1 and iPP/DES1 at a cooling rate of 10 °C min^{-1}

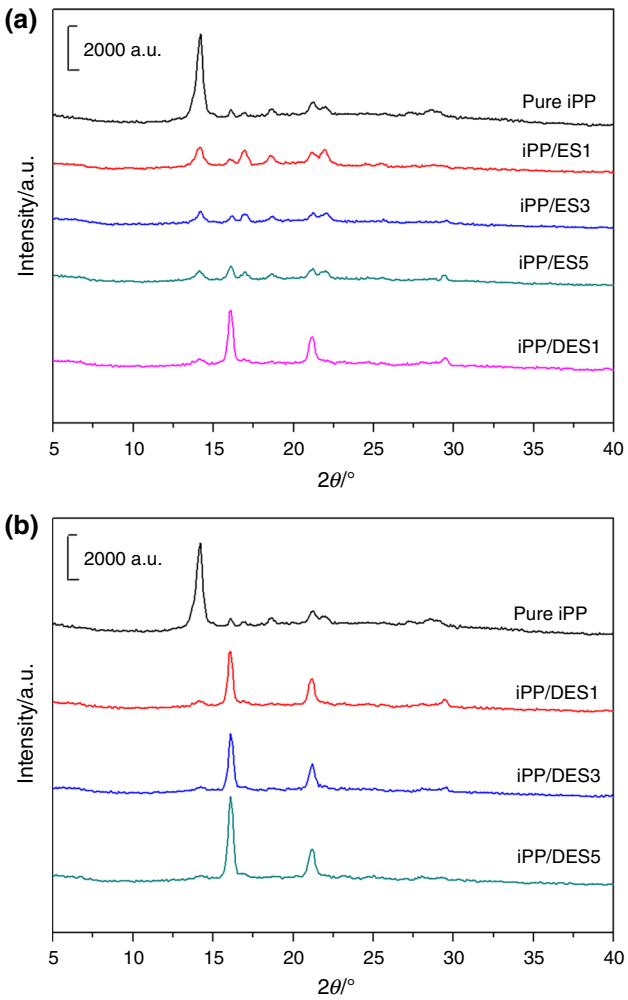

Fig. 5 WAXD profiles of various samples

Fig. 5b. The K_β values were calculated and are given in Table 1. As shown in Table 1, the K_β value of iPP nucleated by DES further increased with increasing content of DES. With 5 mass% DES, a high K_β value of 87% could be obtained, indicating that the DES prepared in current research had high β-form nucleating ability compared with the β-form nucleating agent reported previously [13, 16, 19]. At the same time, the abundant sustainable resource of the eggshell makes the DES of lower price.

Crystallization and melting behaviors of iPP nucleated by DES with various scan rates

The melting behaviors of neat iPP, iPP incorporated with 5 mass% ES and iPP nucleated by 5 mass% DES with various heating rates are shown in Fig. 6. To eliminate the thermal history, all samples were maintained at 190 °C for 3 min and then cooled to 40 °C with a cooling rate of 10 °C min^{-1} before evaluating the melting behaviors with various scanning rates. Multiple melting peaks with one main melting peak at around 161–166 °C, corresponding to the melting of the α-phase, could be found for neat iPP. For iPP incorporated with 5 mass% ES, two melting peaks could be also observed. For iPP nucleated by DES, the intensity of the low-temperature melting peak relating to the melt of β-form crystals increased, while that of the high-temperature melting peak decreased with an increase in the heating rate. It has been observed that a critical cooling temperature (T_r*) has to be reached for the β*a*-recrystallization tendency to appear previously [26]. According to previous measurements, $T_r^* \approx 105$ °C. In the current work, the cooling temperature used (50 °C) was far below the T_r*. Therefore, the melting of samples cooled to 50 °C after crystallization involves a complex process with three partially overlapping processes [β-melting, recrystallization in the α-modification (βa-recrystallization), and α-melting]. Therefore, the overlapping processes could be clearly observed for iPP nucleated by DES. However, for neat iPP and iPP incorporated with 5 mass% ES samples, this melt phenomenon could not be clearly seen, which may be due to the fact that the α-form crystals formed during the cooling process for neat iPP and iPP incorporated with 5 mass% ES samples.

The nonisothermal crystallization curves with various cooling rates and subsequent melting behavior with a heating rate of 10 °C min^{-1} for various samples are shown in Fig. 7. As shown in Fig. 7a, c, e, for all the samples, increasing cooling rate made crystallization temperature peaks shift to low temperature. At a given crystallization temperature, crystallization temperature peak for iPP nucleated by DES was obviously higher than those for pure iPP and iPP incorporated with 5 mass% ES. The faster the cooling rate, the higher the crystallization peak for iPP nucleated by DES. For example, at a cooling rate of

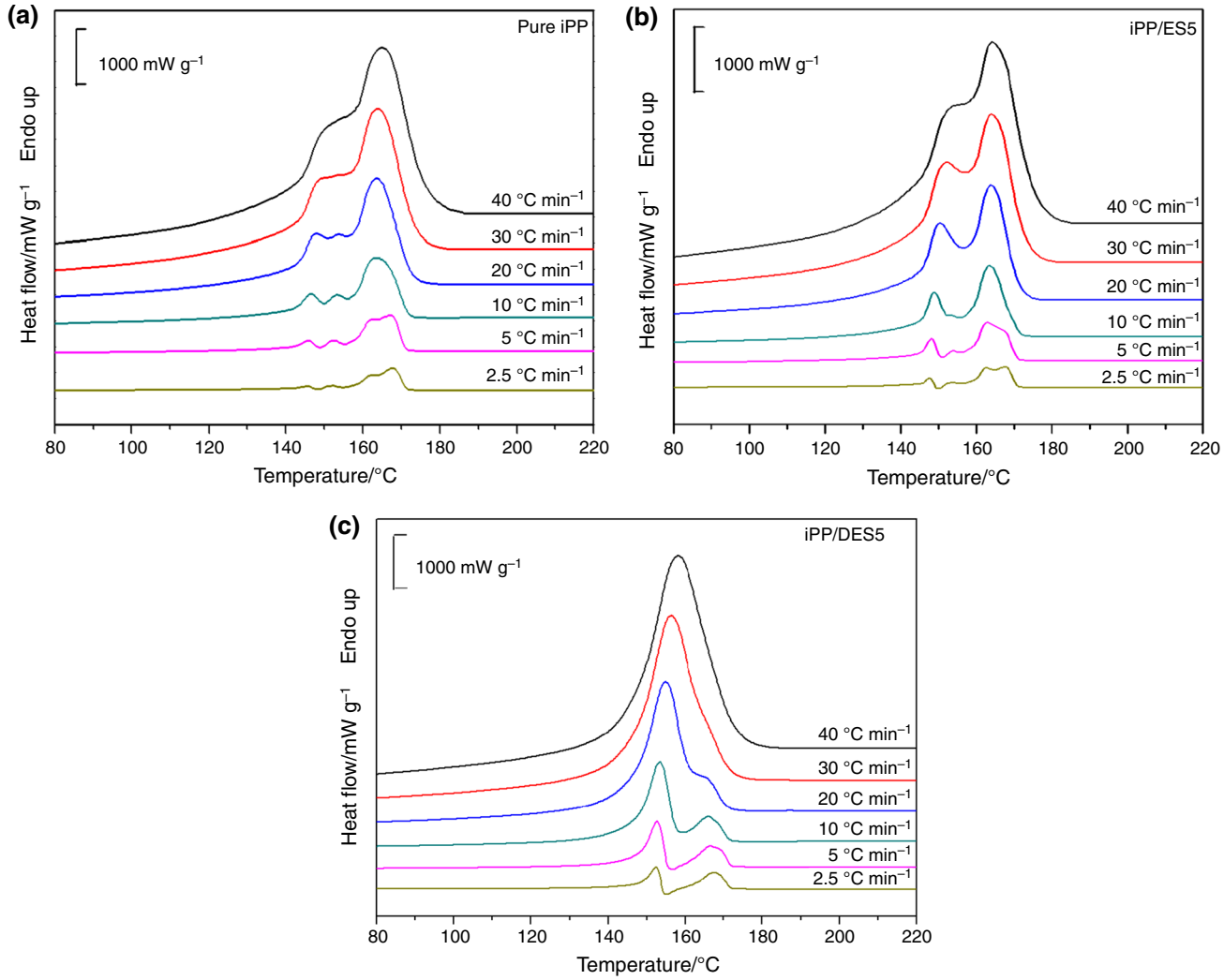

Fig. 6 DSC melting plots of iPP, iPP incorporated with 5 mass% ES and iPP nucleated by 5 mass% DES with heating rates of 2.5, 5, 10, 20, 30, 40 °C min^{-1}

2.5 °C min^{-1}, the crystallization temperature peak increased by 10 °C for iPP nucleated by DES compared with neat iPP. It increased by 20 °C when a cooling rate of 40 °C min^{-1} was used. Moreover, as shown in Fig. 7b, d, f, multiple melting behaviors for all samples can be clearly observed. The neat iPP and iPP incorporated with 5 mass% ES samples showed typical melting characteristic of the α-phase, which suggested that main α-form crystals formed under these nonisothermal crystallization conditions. For iPP nucleated by DES, the typical melting characteristic of the β-phase can be observed, indicating main β-form crystals formed. With increasing cooling rates, the β-form crystals melting peaks of all samples shifted to low temperature. For pure iPP and iPP incorporated with 5 mass% ES samples, the melting peaks of both α-form and β-form crystals shifted to high temperature with decreasing cooling rates, which was due to the fact that under slower cooling rate, more perfect crystals can be formed. However, for iPP nucleated by DES, only the melting peaks of β-form crystals shifted to high temperature with decreasing cooling rates, while the melting peaks of α-form crystals remained almost unchanged. Since the main β-form crystals formed during the nonisothermal crystallization process in the presence of DES, the α-form crystals formed mainly as a result of melting–recrystallization–melting processes, which had little dependence on the nonisothermal crystallization processes. Hence, the melting peaks of α-form crystals derived from the melting–recrystallization–melting processes were almost the same.

Crystallization and melting behaviors of iPP nucleated by DES with multiple scans

Figure 8 demonstrates the crystallization and subsequent melting plots of neat iPP, iPP incorporated with 5 mass% ES and iPP nucleated by DES under multiple scanning

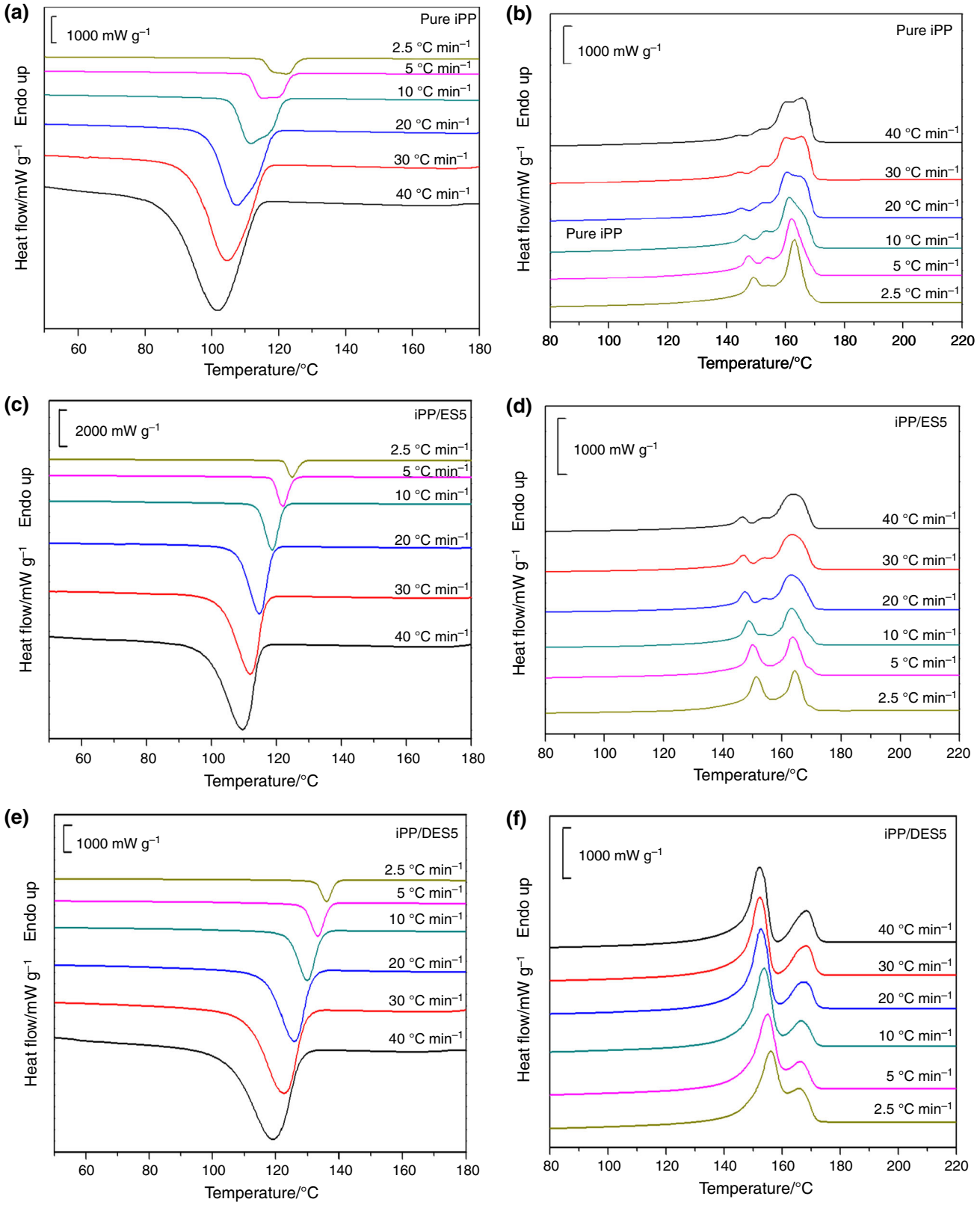

Fig. 7 Crystallization (**a**, **c**, **e**) and melting (**b**, **d**, **f**) plots of iPP, iPP incorporated with 5 mass% ES and iPP nucleated by 5 mass% DES with cooling rates of 2.5, 5, 10, 20, 30, 40 °C min^{-1} and subsequent heating rate of 10 °C min^{-1}

conditions with various melt temperatures (T_{melt}). As shown in Fig. 8, the T_{melt} in the range of 190–250 °C caused no clear effect on the melting and enthalpy of crystallization of neat iPP, iPP incorporated with 5 mass% ES and iPP nucleated by DES. Only the crystallization peak of the sample slightly shifted to high temperature with a decrease in T_{melt}. For the T_{melt} in the range from 190 to 250 °C, neat iPP and iPP incorporated with 5 mass% ES mainly crystallized in α-form crystals; however, iPP nucleated by DES mainly crystallized in β-form crystals. These results indicate that the T_{melt} in the range from 190 to 250 °C does not affect the β-form nucleating ability and nucleating efficiency of the prepared β-form nucleating agent and still has high β-form nucleated efficiency in a wide temperature range of melting processing, which can be applied to fabricate the high-performance β-iPP blends with engineering plastic such as polyamide 6, polyethylene terephthalate at higher melt processing temperature [27, 28].

Isothermal crystallization and melting characteristics of iPP nucleated by DES

It is well known that isothermal crystallization temperature plays a significant role in the polymorphs behavior of a semicrystalline polymer [29]. The polymorphs with α-form and β-form crystals for iPP have been widely investigated previously, and crystallization kinetics was found to be the main fact in affecting polymorphs between α-form and β-form crystals for iPP [13]. Therefore, it is interesting to estimate the effect of isothermal crystallization temperature on the polymorphs structure of iPP nucleated by DES. The isothermal crystallization behaviors of the typical samples of neat iPP, iPP incorporated with 5 mass% ES and iPP nucleated by DES were investigated. Firstly, the isothermal crystallization of neat iPP and iPP incorporated with 5 mass% ES has been determined in a crystallization temperature range from 127.5 to 135 °C. Figure 9a shows the exotherms of crystallization for neat iPP. With increasing crystallization temperature, the exotherms of crystallization shifted right side along the X-axis. The induction time and the exotherm width increased, suggesting that the crystallization rate decreased with a decrease in undercooling (ΔT). This isothermal crystallization behavior could also be observed for iPP incorporated with 5 mass% ES sample as shown in Fig. 9c. However, for iPP nucleated by DES sample, the addition of DES caused a critical influence on the crystallization characteristics of iPP. Addition of DES into iPP matrix leads to great enhancement in the crystallization rate as shown in Fig. 9e. The practically available crystallization temperature range increased by 10 °C, from 127.5 to 137.5 °C, indicating the high nucleating ability of the DES.

Integrating crystallization exotherm curves, the conversion level (t_i) versus time (t) could be obtained. Crystallization rates of the samples could be further discussed based on the $t_{0.1}$ values, which corresponds to the time when conversion degree of crystallization reached 10% [23]. Then, $1/t_{0.1}$, representing the global crystallization rate parameter, was used [23]. The crystallization rates of various samples at different crystallization temperatures were further evaluated by the $1/t_{0.1}$ values. As shown in Fig. 10, when the undercooling conditions altered, pronounced effect on $1/t_{0.1}$ values can be found. In particular, the addition of DES resulted in great enhancement of the overall rate of crystallization in the iPP composites, although the relative enhancement was not pronounced and tended to level off at contents up to 3 mass% of DES.

The melting behavior of neat iPP, iPP incorporated with 5 mass% ES and iPP nucleated by DES was studied through subsequently heating the crystallized samples at the same heating rate of 10 °C min^{-1}, and the corresponding DSC heating curves are shown in Fig. 9. Apparently, the crystallization temperature played an important role in affecting the melting behavior of the iPP matrix after isothermal crystallization completed. Figure 9b shows the melting curves of neat iPP at various crystallization temperatures after isothermal crystallization. The melting curve of neat iPP had two melting endotherms, and iPP crystallized mainly in α-form crystal at various crystallization temperatures. Moreover, all melting point temperatures increased with an increase in crystallization temperature as a result of the fact that the enthalpy contribution of the melting of the much more perfect crystals could be formed under the higher crystallization temperature conditions. Very similar melting characteristics of iPP incorporated with 5 mass% ES can also be observed. These results can be further identified by WAXD experiments shown in Fig. 11. Moreover, it should be noted that for neat iPP the intensity of (110) crystal plane of α-form is very large. For all the samples, orientation effect could be elucidated due to the fact that the prepared process for all samples only involved melt compression molding at 180 °C. In fact, additives used during polymerization, catalyst residues, blends and substrates, etc. may all affect the crystallization process of iPP, which made the crystal preferably grow along certain axis [30]. For example, for XRD patterns of iPP/polyamide 6 blends, the intensity of (040) crystal planes of α-form is very large [31]. However, the exact reason for this phenomenon is not clear.

However, for the iPP nucleated by DES sample in Fig. 9f, the melting characteristics are very different depending on the different crystallization temperature. One main melting peak derived from main β-form crystals at around 158 °C can be found in the melting plots of samples isothermally crystallized at a T_c range of 137.5–140 °C,

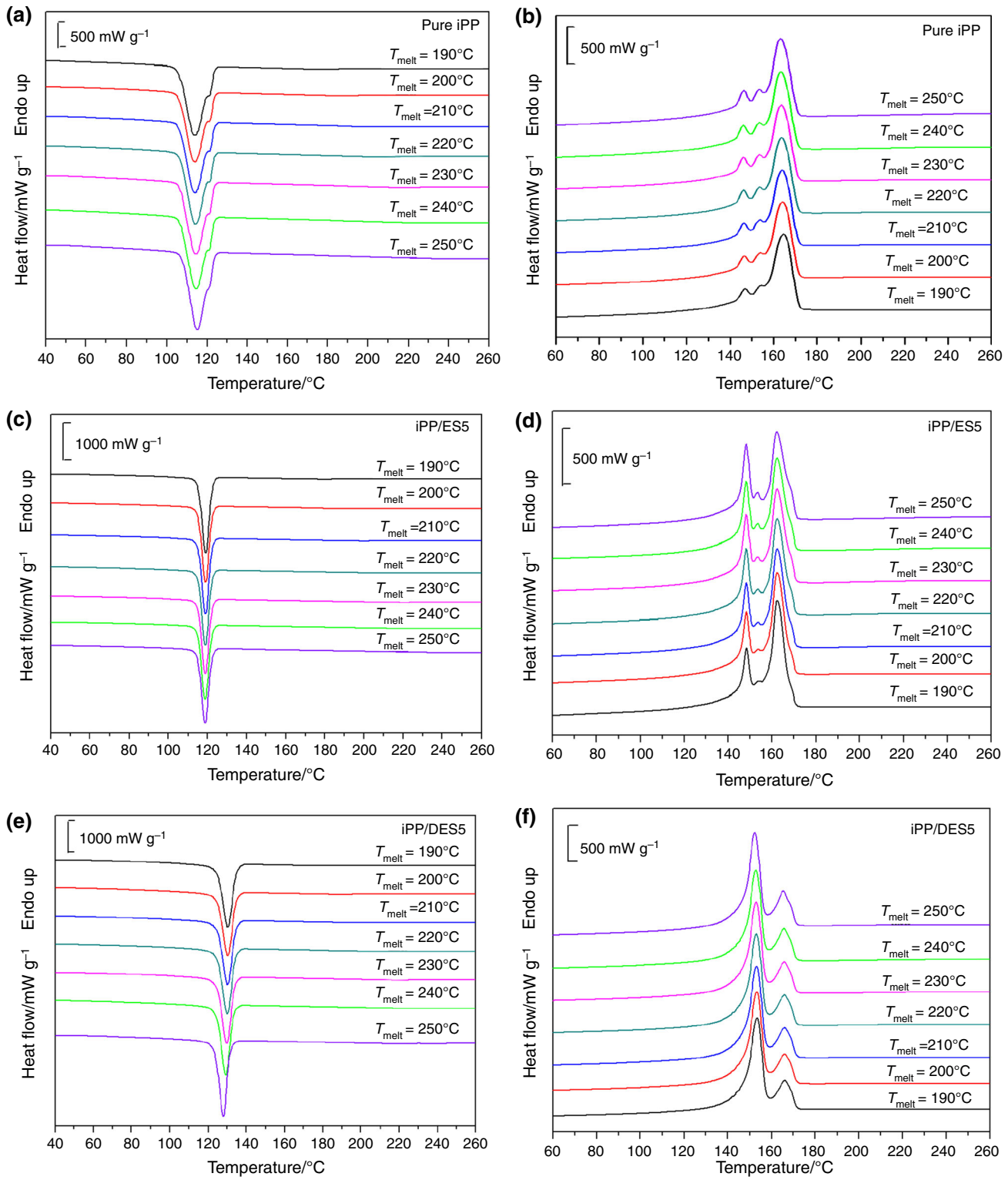

Fig. 8 Crystallization and melting plots of iPP, iPP incorporated with 5 mass% ES and iPP nucleated by 5 mass% DES with various T_{melt} (cooling and heating rates of 10 °C min^{-1})

and the K_β value in the iPP calculated from Eq. (1) by WAXD was >50% as shown in Fig. 11c. This result confirmed the preferred β-form crystals growth during the complete crystallization process. With an increase in T_c up to 140 °C, the main endotherm relating to the α-form crystals could be observed and gradually heightened, which

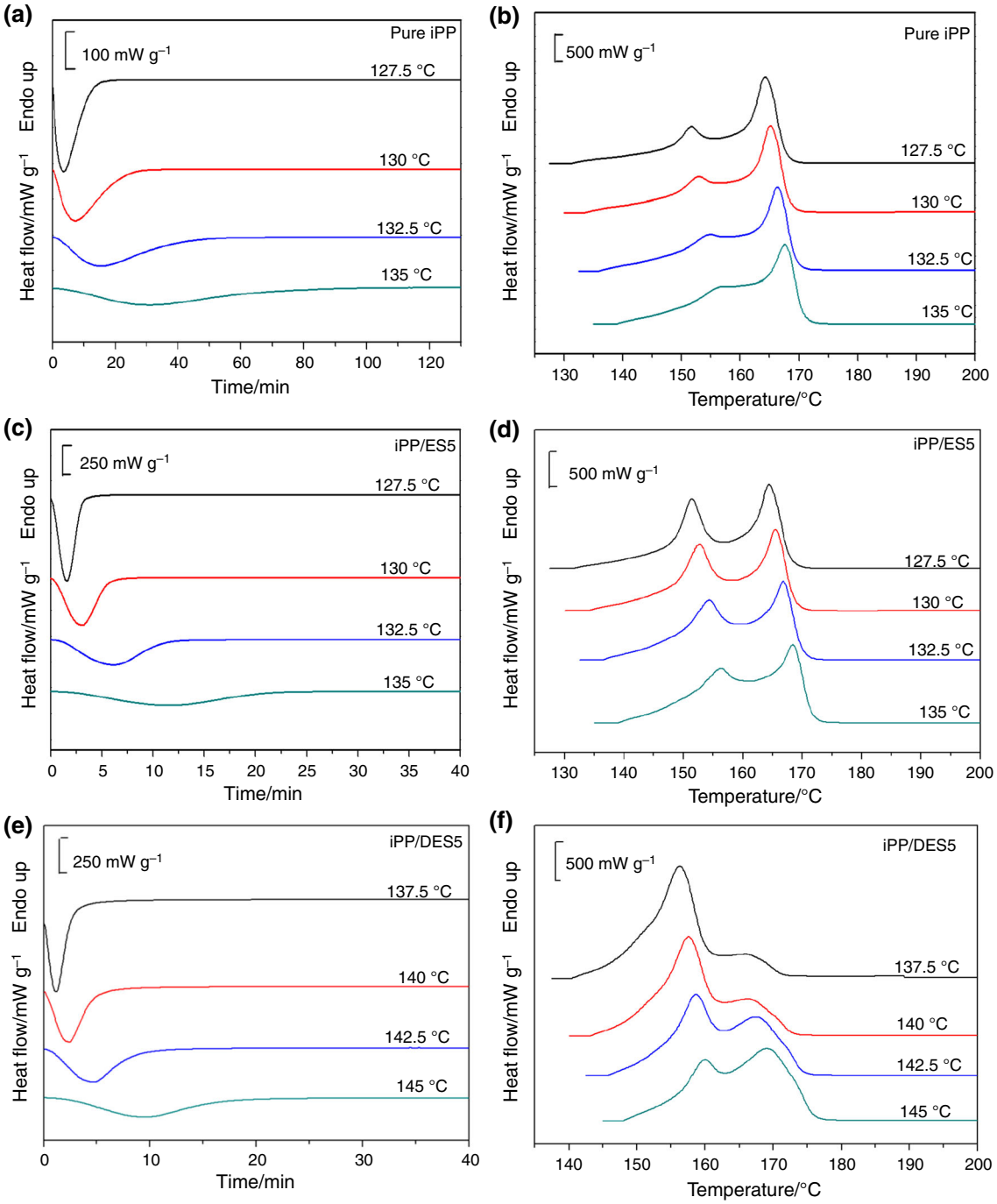

Fig. 9 DSC plots of isothermal crystallization and subsequent melting behavior for various samples with a heating rate of 10 °C min^{-1}

indicated that the preferred α-form crystals formed under the isothermal crystallization conditions. These results clearly indicated that DES was a temperature-dependent selective nucleating agent under isothermal crystallization conditions. The higher the isothermal crystallization temperatures, the smaller the proportions of β-form modification obtained. In other words, even only incorporated with a β-form nucleator, competitive crystal growth between the α-form and β-form crystals still existed under the different isothermal crystallization conditions. The thermodynamics and kinetics factors of the crystallization of iPP nucleated by DES played important roles in the temperature-dependent selective nucleating phenomenon. Both α-form and β-form crystals of iPP had the similar threefold helical conformation of macromolecule chains. The growth rate of β-form crystals of iPP was higher than that of α-form crystals of iPP in the crystallization temperature range of 100–140 °C; 135 °C was considered to be the most

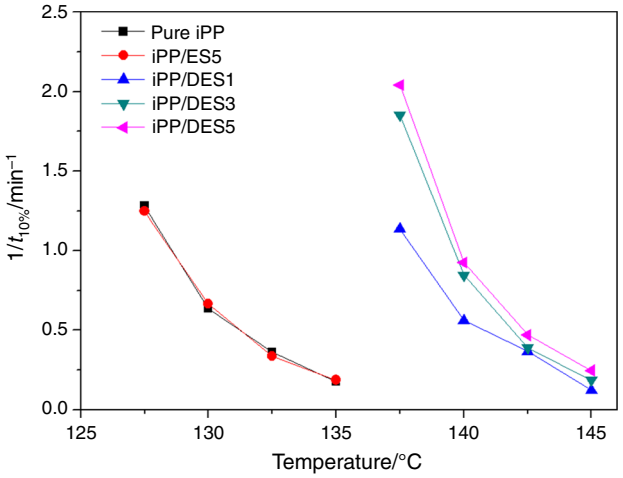

Fig. 10 Crystallization rate versus crystallization temperature for various samples

preferable crystallization temperature to develop the β-form crystals [18]. Generally, crystallization process with a negative enthalpy was exothermic. The enthalpy of 100% α-form crystals of iPP was 177 J g^{-1}, while that of 100% β-form crystals of iPP was 168.5 J g^{-1} [22]. From the thermodynamical point, due to a lower enthalpy, it was more preferable to develop α-form crystals. In addition, α-form crystals of iPP have faster growth rate than β-form crystals of iPP at relatively high crystallization temperature due to the supercooling, in particular at a crystallization temperature above 140 °C. Moreover, increasing the levels of DES into iPP matrix may increase nucleating sites and therefore result in enhancement of the crystallization rate as well as the crystallization exothermic heat. The crystallization exothermic heat could not diffuse out timely, which resulted in an increase in crystallization temperature locally [18]. These factors may explain the reason that the crystallization of the β-form crystals was slow at relatively high crystallization temperature, while the α-form crystals seemed to be more stable and kinetically preferable. Therefore, the α-form crystals predominated with an increase in the crystallization temperature in iPP nucleated by DES. In previous work, Molnár and Menyhárd [32] reported separation of simultaneously developing

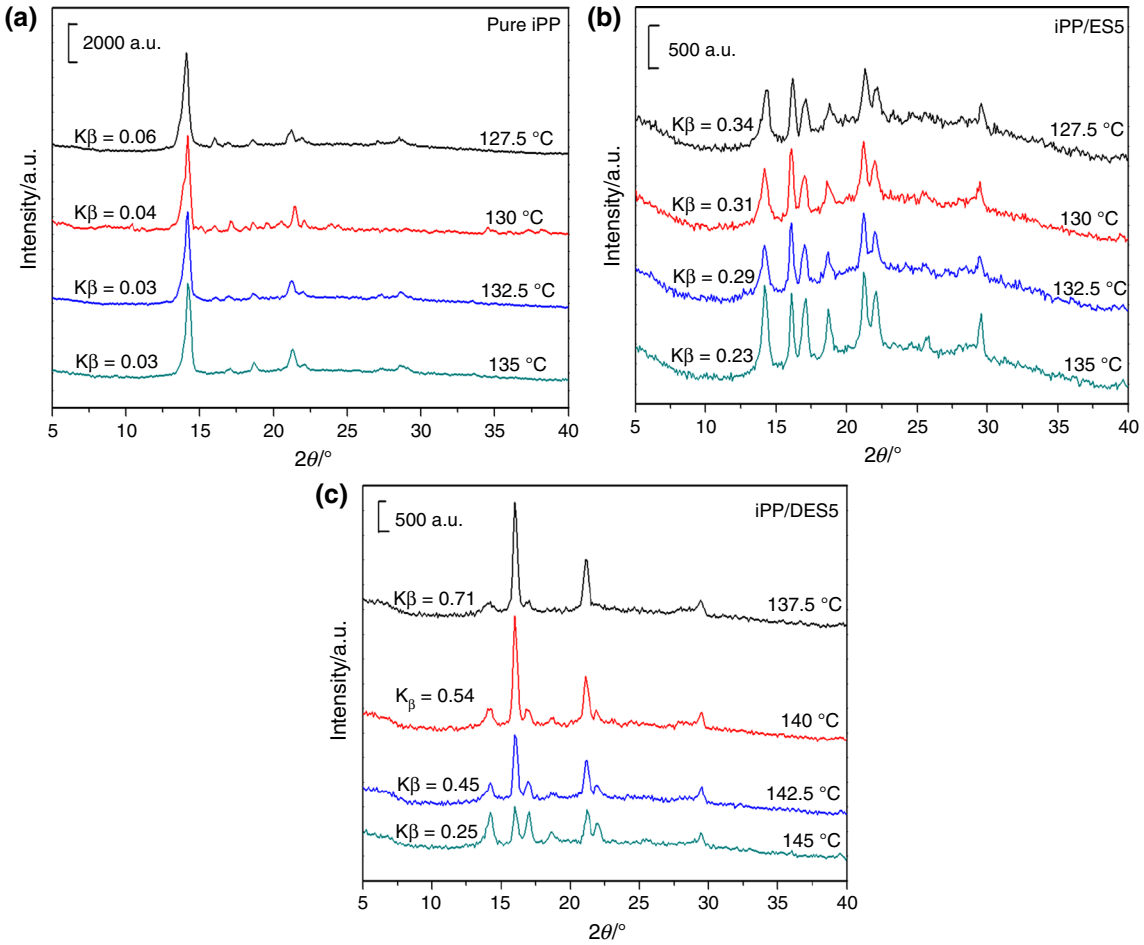

Fig. 11 WAXD profiles of various isothermally crystallized samples

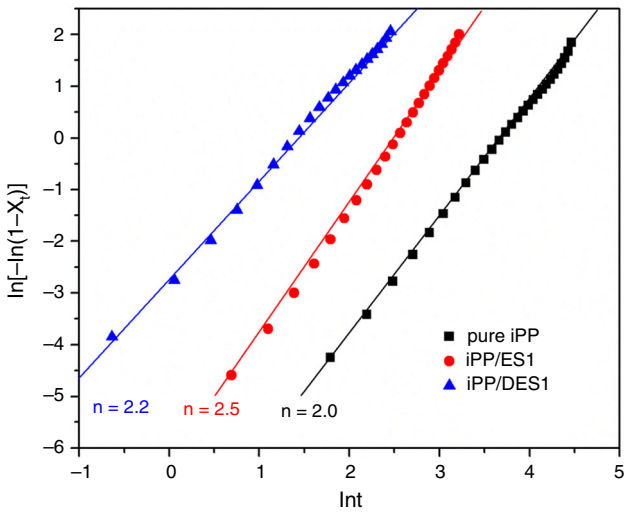

Fig. 12 Avrami plots for the samples of neat iPP and iPP/ES1 isothermally crystallized at 135 °C and sample of iPP/DES1 isothermally crystallized at 140 °C

polymorphic modifications by stepwise crystallization technique in nonisothermal calorimetric experiments. Moreover, it was reported that the incorporation of different kinds of nucleating agent into polymer matrix can induce different kinds of crystals to tailor the mechanical properties of iPP, for example, α-form crystals and β-form crystals nucleating agents in iPP matrix [22, 23]. It is important to develop novel single nucleating agent, which has selective dual nucleating ability by only tuning the crystallization temperature. Therefore, the DES prepared in current work exhibited selective dual nucleating ability during isothermal crystallization process, which can be used to fabricate ideal iPP composites with controlled proportional α-form crystals and β-form crystal content via a simple and convenient approach. Such iPP composite may have great potential industrial interest.

The Avrami equation (Eq. 2) is frequently employed to analyze the isothermal crystallization kinetics of polymers. The Avrami parameter n can be obtained from the slopes. Figure 12 shows such plots for the samples of neat iPP and iPP/ES1 isothermally crystallized at 135 °C and sample of iPP/DES1 isothermally crystallized at 140 °C. The values of n are also shown in Fig. 12. The value of n fluctuates within the range of 2.0–2.5 and is almost irrespective of the addition of ES and DES, indicating that the addition of ES and DES may not change the crystallization mechanism of iPP.

Conclusions

The surface modification of sustainable eggshell powder with PA to form an effective β-form nucleating agent for iPP was successfully realized by the reaction between PA and the Ca^{2+} on the surface of eggshell powder. The DES demonstrated high β-form nucleating efficiency. The K_β values could reach 79% with only addition of 1 mass% DES. The K_β value of iPP nucleated by DES further increased with increasing content of DES. Moreover, the results of multiple scans indicated that the T_{melt} in the range from 190 to 250 °C did not affect the β-form nucleating ability and nucleating efficiency and still exhibited high β-form nucleating efficiency. The isothermal crystallization results suggested that DES had dual nucleating ability for inducing iPP crystallization. Main α-form crystals or β-form crystals formed at T_cs of 145 or 137.5 °C, respectively. In other words, the ratio of α-form crystals to β-form crystals could be tailored by simply changing isothermal crystallization temperatures. The changes in polymorphs behavior were strongly related to the thermodynamics and kinetics factors of crystallization.

Acknowledgements This work is supported by government of Taian city and Science and Technology Department of Shandong Province (2015ZDZX11002). Part of this work is supported by program of International S & T Cooperation (2013DFR50880), program of Cooperation of Hubei Province and Chinese Academy of Sciences, Jilin Province Science and Technology Agency (20160204030GX), and program of Changchun Municipal Scientific and Technologic Development (16SS16). Part of this work is supported by Startup Foundation for Doctors of Jilin Jianzhu university (861107).

References

1. Kang DJ, Pal K, Park SJ, Bang DS, Kim JK. Effect of eggshell and silk fibroin on styrene–ethylene/butylene–styrene as bio-filler. Mater Des. 2010;31:2216–9.
2. Hassan TA, Rangari VK, Rana RK, Jeelani S. Sonochemical effect on size reduction of $CaCO_3$ nanoparticles derived from waste eggshells. Ultrason Sonochem. 2013;20:1308–15.
3. Torres FG, Troncoso OP, Montes MR. The effect of temperature on the mechanical properties of a protein-based biopolymer network. J Therm Anal Calorim. 2013;111:1921–5.
4. Schaafsma A, Pakan I, Hofstede GJH, Muskiet FK, Van DerVeer E, De Vries PJF. Mineral, amino acid, and hormonal composition of chicken eggshell powder and the evaluation of its use in human nutrition. Poult Sci. 2000;79:1833–8.
5. Zheng W, Li X, Yang Q, Zeng QG, Shen X, Zhang XY, Liu J. Cu(II) from aqueous solution by carbonate hydroxylapatite derived from eggshell waste. J Hazard Mater. 2007;147:534–59.
6. Ke YT, Garg B, Ling YC. Waste chicken eggshell as low-cost precursor for efficient synthesis of nitrogen-doped fluorescent carbon nanodots and their multi-functional applications. RSC Adv. 2014;4:58329–36.
7. Hassan TA, Rangari VK, Jeelani S. Value-added biopolymer nanocomposites from waste eggshell-based $CaCO_3$ nanoparticles as fillers. ACS Sustain Chem Eng. 2014;2:706–7.
8. Rahman MM, Netravali AN, Tiimob BJ, Rangari VK. Bioderived "green" composite from soy protein and eggshell nanopowder. ACS Sustain Chem Eng. 2014;2:2329–37.
9. Bootklad M, Kaewtatip K. Biodegradation of thermoplastic starch/eggshell powder composites. Carbohydr Polym. 2013;97:315–30.

10. Padden FJ, Keith H. Spherulitic crystallization in polypropylene. J Appl Phys. 1959;130:1479–84.
11. Lotz B. A new ε crystal modification found in stereodefective isotactic polypropylene samples. Macromolecules. 2014;47: 7612–24.
12. Varga J, Stoll K, Menyhárd A, Horváth Z. Crystallization of isotactic polypropylene in the presence of a β-nucleating agent based on a trisamide of trimesic acid. J Appl Polym Sci. 2011;12:1469–80.
13. Zhan KJ, Yang W, Yue L, Xie BH, Yang MB. MWCNTs supported *N*,*N*′-dicyclohexyl-1,5-diamino-2,6-naphthalenedicarboxamide: a novel β-nucleating agent for polypropylene. J Macromol Sci Part B Phys. 2012;51:2412–22.
14. Bao RY, Cao J, Liu ZY, Yang W, Xie BH, Yang MB. Towards balanced strength and toughness improvement of isotactic polypropylene nanocomposites by surface functionalized graphene oxide. J Mater Chem A. 2014;2:3190–9.
15. Lin ZD, Zhang ZS, Mai KC. Preparation and properties of eggshell/β-polypropylene bio-composites. J Appl Polym Sci. 2012;125:61–6.
16. Menyhárd A, Varga J, Molnár G. Comparison of different β-nucleators for isotactic polypropylene, characterization by DSC and temperature-modulated DSC (TMDSC) measurements. J Therm Anal Calorim. 2006;83:625–30.
17. Kang J, Peng HM, Wang B, Chen ZF, Li JP, Chen JY, Cao Y, Li HL, Yang F, Xiang M. Comparative study on the crystallization behavior of β-isotactic polypropylene nucleated with different β-nucleation agents—effects of thermal conditions. J Appl Polym Sci. 2014;131:40115–26.
18. Cai ZW, Zhang Y, Li JQ, Shang YR, Huo H, Feng JC, Funari SS, Jiang SC. Temperature-dependent selective crystallization behavior of isotactic polypropylene with a b-nucleating agent. J Appl Polym Sci. 2013;128:628–35.
19. Zhao SC, Cai Z, Xin Z. A highly active novel β-nucleating agent for isotactic polypropylene. Polymer. 2008;49:2745–54.
20. Mani MR, Chellaswamy R, Marathe YN, Pillai VK. New understanding on regulating the crystallization and morphology of the β-polymorph of isotactic polypropylene based on carboxylate-alumoxane nucleating agents. Macromolecules. 2016; 49:2197–205.
21. Hu X, Geng CZ, Yang GG, Fu Q, Bai HW. Synergetic effects of a matrix crystalline structure and chain mobility on the low temperature toughness of polypropylene/ethylene–octene copolymer blends. RSC Adv. 2015;5:54488–96.
22. Naffakh M, Marco C, Ellis G. Novel polypropylene/inorganic fullerene-like WS_2 nanocomposites containing a β-nucleating agent: dynamic crystallization and melting behavior. J Phys Chem B. 2011;115:10836–43.
23. Naffakh M, Marco C, Ellis G. Novel polypropylene/inorganic fullerene-like WS_2 nanocomposites containing a β-nucleating agent: isothermal crystallization and melting behavior. J Phys Chem B. 2012;116:1788–95.
24. Zhang C, Wang B, Yang J, Ding D, Yan X, Zheng G, Dai K, Liu C, Guo Z. Synergies among the self-assembled β-nucleating agent and the sheared isotactic polypropylene matrix. Polymer. 2015;60:40–9.
25. Avrami M. Kinetics of phase change. I. General theory. J Chem Phys. 1939;7:1103–12.
26. Varga J. Melting memory effect of the β-modification of polypropylene. J Therm Anal Calorim. 1986;31:165–72.
27. Yousfi M, Livi S, Dumas A, Crépin-Leblond J, Greenhill-Hooper M, Duchet-Rumeau J. Ionic compatibilization of polypropylene/polyamide 6 blends using an ionic liquids/nanotalc filler combination: morphology, thermal and mechanical properties. RSC Adv. 2015;5:46197–205.
28. Zhao ZG, Yang Q, Xi ST, Kong MQ, Huang YJ, Liao X. New understanding of the hierarchical distribution of isotactic polypropylene blends formed by microinjection-molded poly(-ethylene terephthalate) and β-nucleating agent. RSC Adv. 2015;5:61127–36.
29. Li Y, Han CY, Bian YJ, Dong QL, Zhao HW, Zhang X, Xu MZ, Dong LS. Miscibility, thermal properties and polymorphism of stereocomplexation of high-molecular-weight polylactide/poly(D,L-lactide) blends. Thermochim Acta. 2014;580:53–62.
30. Langhe DS, Hiltner A, Baer E. Effect of additives, catalyst residues, and confining substrates on the fractionated crystallization of polypropylene droplets. J Appl Polym Sci. 2012;125:2110–20.
31. Ou BL, Ou YJ, Li DX, Jing B, Gao Y, Zhou ZH, Liu QQ. Isothermal crystallization and melting behaviors of nano TiO_2-modified polypropylene/polyamide 6 blends. Polym Compos. 2012;33:1054–63.
32. Molnár J, Menyhárd A. Separation of simultaneously developing polymorphic modifications by stepwise crystallization technique in non-isothermal calorimetric experiments. J Therm Anal Calorim. 2016;124:1463–9.